LONG TERM STORAGE OF SOLAR ENERGY BY INJECTING HOT WATER INTO GROUNDWATER AQUIFERS

by

David B. Reed

Agricultural Engineering

Submitted in Partial Fulfillment of the Requirements of the University Undergraduate Fellows Program

1976 - 1977

Approved by:

Donald L. Reddell

Donald L. Reddell

May 1977

ABSTRACT

The energy shortage has caused increased interest in alternate energy sources such as solar energy. Solar energy is most efficiently used in the form of hot water which can be used for space heating. The problem of using solar energy in the form of hot water is that no effective long-term hot water storage is available. The proposed method of storing this water is by injecting this water into groundwater aquifers. To effectively design such a system, models of solar energy collection and hot water injection into groundwater aquifers is needed.

A computer model to simulate solar energy collection by heating water was used to develop curves that show the amount of water that could be heated at a given location. A computer model that simulates hot water injection into a groundwater aquifer must combine mass flow and heat transfer properties simultaneously. After writing a computer program that models this process, properties that effect recovery efficiencies can be studied.

ACKNOWLEDGEMENTS

I would like to thank Dr. Donald L. Reddell, my faculty advisor, and Elston Grubaugh, a graduate student in Agricultural Engineering, for their help in conducting my research and preparing this report. I also thank Paula Parma who has had the task of typing my report.

TABLE OF CONTENTS

LIST OF TABLES

LIST OF FIGURES

INTRODUCTION

Energy is currently an area of major concern in the United States and the world. With the depletion of the world's oil and gas reserves, interest in the development and utilization of alternate energy sources such as solar energy has greatly increased. Solar energy, most efficiently utilized in the form of hot water, has tremendous possibilities in the areas of space heating, air conditioning, and greenhouse operations.[1]

Large amounts of clean energy are available by harvesting the sun's rays. This energy is diffuse and leads to large collector areas. This results in increasing energy costs. Technology has not progressed to the point of economical electric power generation by using photovoltaic cells. Currently, the most promising method of using solar energy is heating water by using solar heaters. This hot water can then be used for space heating.

The major drawbacks of using solar energy in the form of hot water are (1) solar energy is intermittent and undependable and (2) storage of large quantities of hot water is difficult. Solar energy is least during winter when space heating requirements are a maximum. Conventional solar heated homes have a hot water storage capacity of about six days. Due to the undependability of solar energy and small storage capacity, an auxiliary system that can handle 100% of the heating requirements of a building is needed for extended periods of cold weather. The only savings is in the reduction of fuel costs by using a solar heater.

---

[1]Modeled after Transactions of the ASAE.

A low cost method of storing hot water for extended periods of time is needed. With this, water could be heated in the summer when solar energy is a maximum and stored. This hot water could be used in the winter for 100% of the heating requirements of a building and eliminate the need for an auxiliary system.

A recently developed method has possibilities of long-term energy storage with hot water. This method involves the injection of hot water into groundwater aquifers where it can be stored for several months. The heat losses will be small due to the insulating effect of the earth. This water could then be pumped back to the surface for use in heating homes. Recovery efficiencies as high as 90% have been calculated for this process.

A solar heater, groundwater aquifer storage system must be studied extensively to determine the most economical and energy efficient system. The amounts of water that can be heated at various times of the year for various locations must be known. Currently, computer programs are available that calculate the available solar energy for a given day and location. With this information, the amount of water that can be heated per day can be calculated for a given solar heater.

To study this system completely, we must know the effects of injecting hot water into a groundwater aquifer. A mathematical (computer) model is needed to simulate this process. The development of a computer model that simulates this process requires combining fluid movement and heat transfer properties simultaneously. With a computer model that traces the movement of hot water as it is injected into a groundwater aquifer, many parameters that effect this process can be studied. The efficiency of this storage can be calculated.

This brings us to the objectives of this study:

1. Develop curves that show the amount of water that can be heated to a given temperature at a specified location.
2. Develop mass flow and heat transfer equations that model the injection of hot water into a groundwater aquifer.
3. Write a computer program to model this process.
4. Calculate efficiencies of energy storage by injecting hot water into a groundwater aquifer at various flowrates, injection temperatures, and aquifer depths as well as continuous injection and pumping cycles.

REVIEW OF LITERATURE

Thermal convection occurring in a dispersed porous media was first studied by Horton and Rogers (1945) and Lapwood (1948). Much information now exists for the case where the porous media is homogeneous and isotropic (Combarnous and Bories, 1975). Castinel and Combarnous (1975) developed some information on heat flow in anisotropic media. Aziz et al. (1973) studied the problem of a hot-fluid industrial plant using deep-lying groundwater. After heat exchanges, the cooled and frequently salty water was reinjected into other parts of an aquifer. The efficiency of the process was shown to be closely correlated with water pumping rates, thermal conductivities of the aquifer layers, and the existence of the thermal convection effect.

The investigation of unsteady-state temperature behavior of production wells is extremely complicated. Only for simple systems can the flow be computed analytically. Gringarten and Sauty (1975) have developed analytical solutions for the case of a recharging-discharging well pair in an infinite, horizontal, homogeneous and isotropic aquifer. In more complex heterogeneous systems, it is necessary to use a simulator for computing potential distributions prior to determining stream lines. Lauwerier (1955) studied the transport of heat in an oil layer.

Natural convection arises as a result of density differences, which in turn are a result of temperature differences. No general solution of the Navier-Stokes equations which will supply spatial temperature variations is available. Although no general solution is feasible, natural convection can be analyzed making various simplifications which yield

accurate results for many practical applications, as shown Gebhart (1961) and Holman (1963).

Rabbimov et al. (1974a) investigated the temperature distribution in accumulation of solar energy in an aquifer. They developed an analytical expression for the temperature distribution. Rabbimov et al. (1974b) also conducted an experimental study of aquifer heating in solar-energy accumulation. Their experimental results indicated that convective heating is more effective than conductive heating by a factor of 40. Meyer and Todd (1973) discussed the possibility of storing waste heat from power plants in heat storage wells. Their rough calculations indicated that 80 to 90 percent of the injected heat could be removed.

DEVELOPMENT OF COMPUTER MODELS

Solar Energy Collection

A computer program that simulated solar energy collection by heating water was available. The system that was modeled consisted of a flat-plate solar collector with a temporary storage tank. The water was heated to a desired temperature and then removed from the system. A diagram of this process is shown in Figure 1.

The solar collector modeled was a sheet and tube type of collector which was 3.28 ft. by 6.56 ft. A cross-section of the solar collector is shown in Figure 2. The storage tank was assumed to be cylindrical in shape with an L/D ratio of 1.0. The tank capacity and surface area were determined by the rate the water moved through the collector, the collector area, and the time increment used for the study. The conductance for the tank was assumed to be 0.273 Btu/ ($hr\text{-}ft^2\text{-}°F$). The pipe from the tank to the collector was 32 ft. The pipe with an effective 2 in. layer of insulation was assumed to be iron with an overall heat conductance of .459 Btu/ ($hr\text{-}ft^2\text{-}°F$).

This computer program took weather and solar radiation data and calculated the radiation intensity on a surface for a given azimuth angle, tilt angle, and location. The ambient temperature was determined. With these values, system heat losses and the temperature of the water as it passed through the solar collector were determined. Various water temperatures to begin the heating cycle were used. By using this data, an expression for the amount of water that could be heated in $gal/day\text{-}ft^2$ could be determined. This will be a function of the temperature that the water began the heating cycle and the temperature the water was heated to.

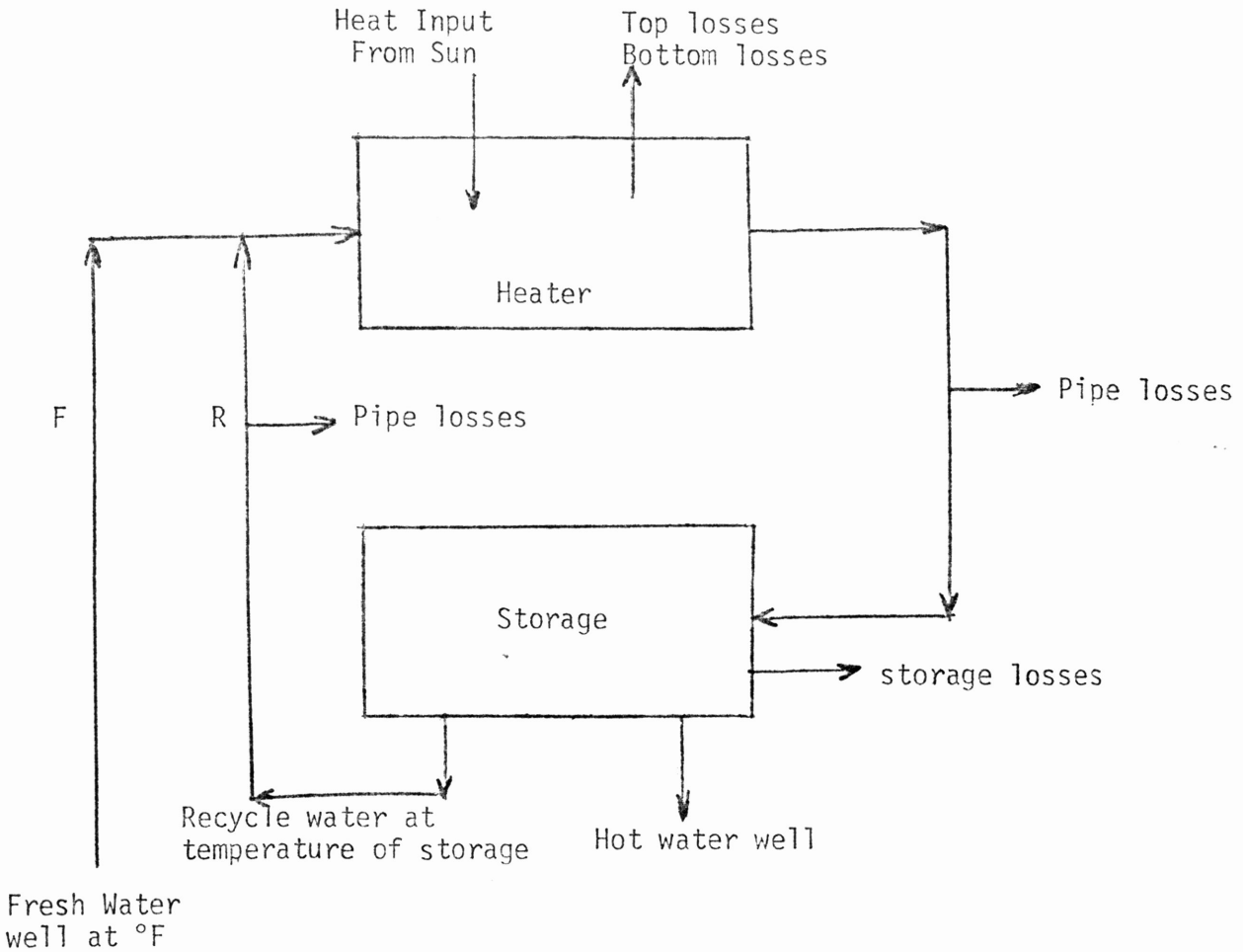

Figure 1. Flat plate solar collector, temporary storage system.

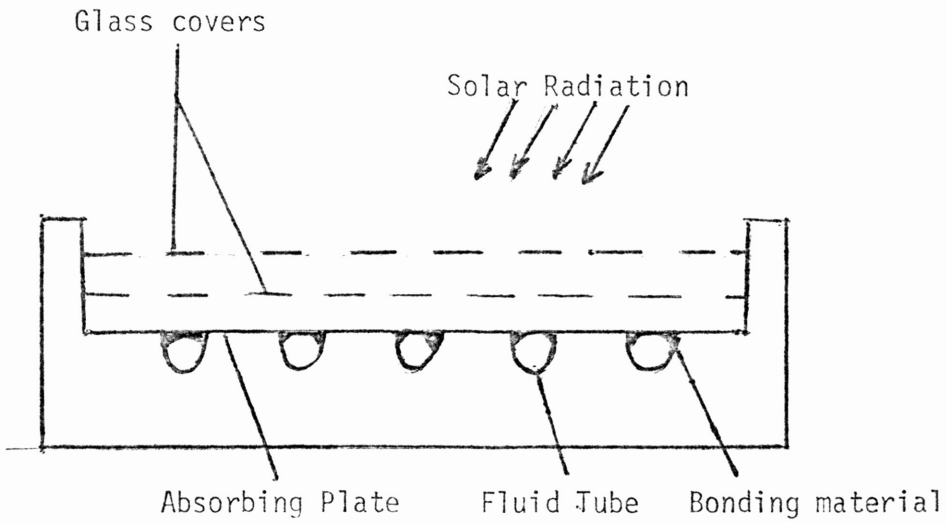

Figure 2. Cross section at a sheet and tube solar collector.

Mass Flow Equations

To determine the movement of hot water as it is injected into a groundwater aquifer, you must first discover the way the water moves through the aquifer. With this information, the resulting temperature can be calculated. To simulate hot water injection, the equations that model this process must be developed.

The development of the equations and computer program, many assumptions were made. For simplicity, we ran a one dimensional analysis. We assumed flow only in the radial direction. The aquifer was assumed to be homogeneous and isotropic. The bedrock and caprock form an impermeable layer below and above the aquifer. The heat losses out the top and bottom were assumed to be proportional to a heat loss coefficient (h) and the temperature differential between the aquifer and the surrounding layers.

In this analysis, we examined a section of the aquifer shaped like a piece of pie. This pie shaped section was further divided at intervals along the radius. This produced an aquifer section like that shown in Figure 3. The radial increments were small next to the well and increased in size as the distance from the well increased.

With the aquifer divided into grids, we will develop the mass flow and heat transfer equations. To determine the mass flow for each grid, a mass balance was run for each grid. The flow is a function of the pressure difference throughout the aquifer. The pressure at the center of each grid is calculated. The computation for the mass flow equation was based on the following relationship:

$$M_{1\to2} - M_{2\to3} = \frac{dMv}{dt} \qquad (1)$$

where $M_{1\to2}$ = mass flow into grid at interface 1

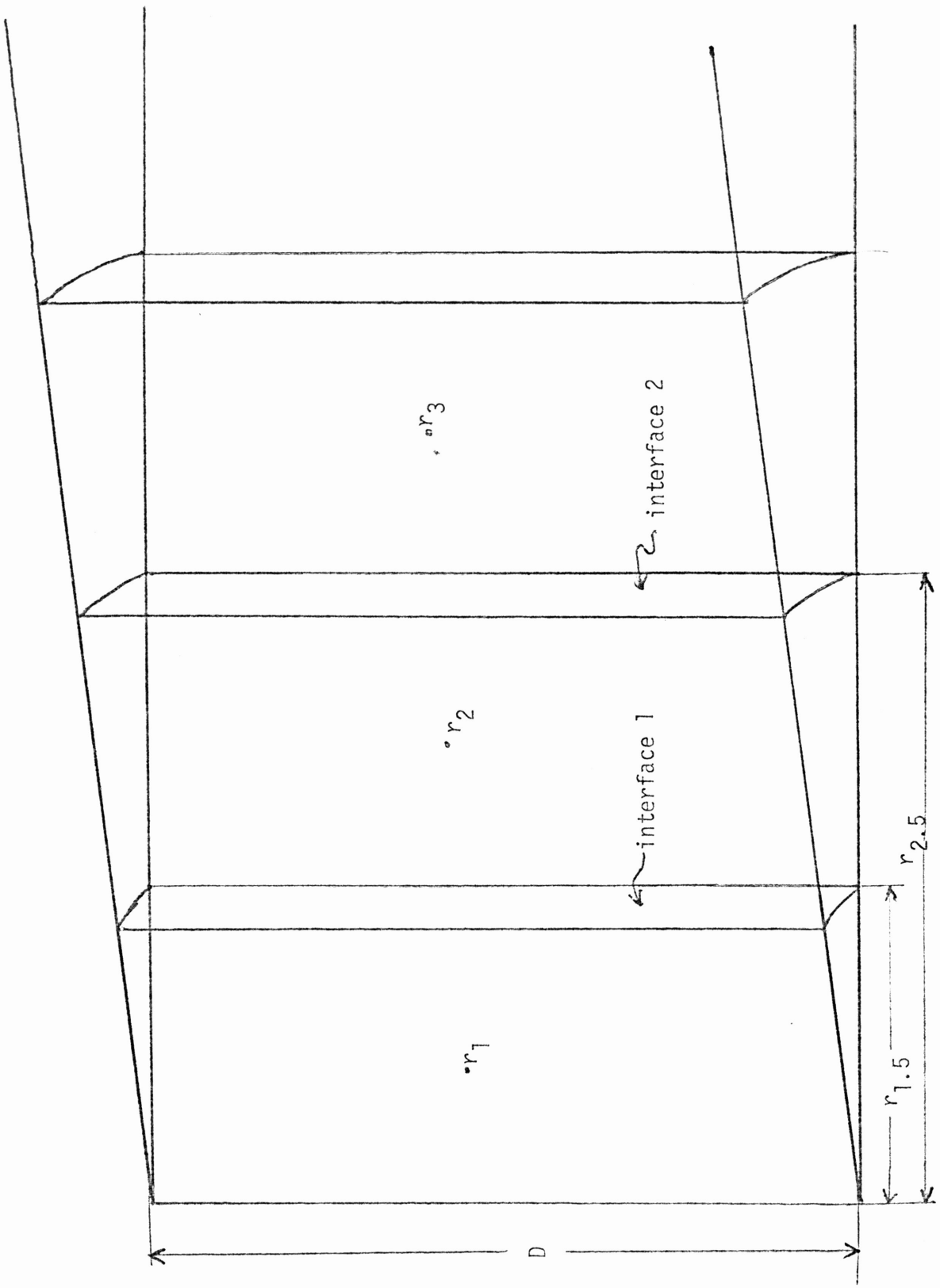

Figure 3. Aquifer divided into grids.

$M_{2\rightarrow 3}$ = mass flow out of grid at interface 2

$\frac{dMv}{dt}$ = change of mass stored in grid section with respect to time.

This sort of mass balance was run for grid 2. Using the properties of the aquifer, Darcy's Law, and the continuity equation, Equation (1) becomes:

$$\frac{\rho_1\rho_2 D_1 D_2 K_1 K_2 \Delta\theta (P_1^{t+\Delta t} - P_2^{t+\Delta t})}{\mu_2\rho_1 D_1 K_1 \ln(\frac{r_2}{r_{1.5}}) + \mu_1\rho_2 D_2 K_2 \ln(\frac{r_{1.5}}{r_1})} -$$

$$\frac{\rho_2\rho_3 K_2 K_3 D_3 D\ \Delta\theta (P_2^{t+\Delta t} - P_3^{t+\Delta t})}{\mu_3\rho_2 D_2 K_2 \ln(\frac{r_3}{r_{2.5}}) + \mu_2\rho_3 D_3 K_3 \ln(\frac{r_{2.5}}{r_3})} =$$

$$\frac{r_2 \Delta\theta \Delta r D_2 \rho_2 \phi_2 (\beta + C_F)(P_2^{t+\Delta t} - P_2^{t}) *}{\Delta t} \qquad (2)$$

where ρ = density $(\frac{M}{L^3})$

D = aquifer depth (L)

K = permeability (L^2)

$\Delta\theta$ = grid angle

μ = Viscosity $(\frac{FT}{L^2})$

P = pressure $(\frac{F}{L^2})$

r = radius (L)

ϕ = porosity

β = density-pressure factor $(\frac{L^2}{F})$

C_F = compressibility factor $(\frac{L^2}{F})$

By putting this in a finite difference scheme, the pressures can be solved directly. The mass flow can be characterized by the pressure

variation. For a more detailed discussion of the derivation, see Appendix A.

Heat Flow Equations

The same procedure was followed in developing heat flow equations. The same grids were used. The heat balance was run using this relationship on grid 2:

$$Jr_{1\to2} - Jr_{2\to3} = \frac{dH_2}{dt} \tag{3}$$

where $Jr_{1\to2}$ = heat flow in at interface 1

$Jr_{2\to3}$ = heat flow out at interface 2

$\frac{dH_2}{dt}$ = change in heat stored in grid 2.

Each heat flow term is composed of two parts. One is conduction. The second is convection. The heat flow due to conduction is

$$r\Delta\theta D\lambda\frac{dT}{dr} \tag{4a}$$

The convection term is

$$-C_F T q r \Delta\theta D \tag{4b}$$

where λ = heat transfer coefficient of aquifer

C_F = bulk heat capacity of fluid

q = flow per unit area

T = temperature at interface between grids

$\frac{dT}{dr}$ = temperature change at grid centers with respect to change in radius.

The fact that the temperature for convection must be calculated at the interface complicates the process. An expression that makes the temperature a function of the grid center temperatures is needed. The

assumption made was that the temperature varied linearly with radius. The temperature T could then be found by knowing the temperature at the grid centers.

By adding this expression to determine the temperature at the interface, problems in solving this system multiply. There is no way to isolate the temperature and obtain a direct solution for the temperature pattern. To solve this, an iteration process was used. An initial guess was made at the temperature. By using this, a temperature was calculated. If this temperature was the same as the guess, then you had the temperature. If they were not the same, the calculated temperature was used to update the coefficients and as the second guess. When the guess was the same as the temperature calculated, you had found the temperature distribution.

For further details, see Appendix B.

RESULTS AND DISCUSSIONS

In studying the amount of water that can be heated by using a solar heater, the water was heated to a set temperature of 130°F. The location chosen for study was Houston, Texas. To determine the amount of water that could be heated by the system, three days in the middle of each month were chosen to make computer runs on. These three days were assumed to represent the collectible solar energy and water heatable during that month.

The amount of water that could be heated for each month was expressed in gal. per day per square foot of collector. The results are shown in Figure 4. These curves show how the water heatable varies by changing the inlet temperature of water into the solar heater. As expected, less water could be heated for the lower inlet temperature. Heating water in stages can be studied by using this figure. The water could be heated from 50°F to 90°F in one stage. Later, the 90°F water could be heated to 130°F and stored. The maximum water heatable is in June, July, and August. The curve of the water heatable looks like a distorted sine wave.

The efficiency of the system decreases as water temperature increases. For an 80°F increase in water temperature from 50°F to 130°F, 1.39 gal. could be heated per day in July. If the efficiency of the solar heater remains the same, 2.78 gal. could be heated from 90°F to 130°F, a 40° rise in temperature. However, Figure 4 shows that only 2.20 gal. could be heated. This indicates the efficiency decreases as the water temperature increases.

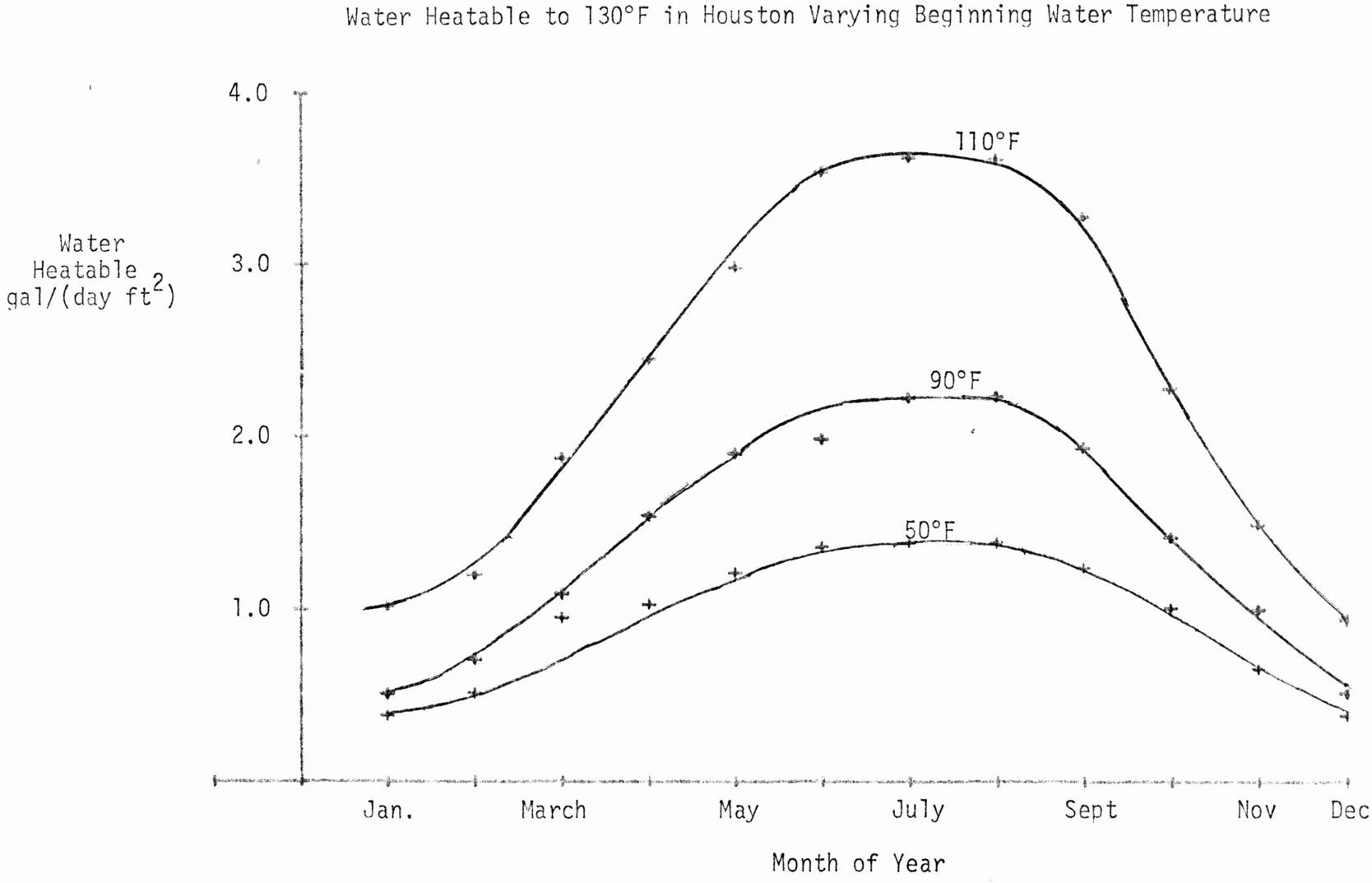

Figure 4. Water Heatable in Houston to 130°F.

A confined aquifer was used as a model. Table 1 lists the physical properties given to the aquifer. In determining the flow in an aquifer, the pressures at the grid centers were determined. The most widely accepted method of pressure calculation is by using the Theis formula. The results comparing the Theis formula and the values calculated are shown in Table 2 and Figure 5. These values are for injecting 100 gpm for a time of 100 hours. The computer values are higher than the Theis values. This small discrepancy could be due to the different boundary conditions. A constant head boundary was imposed at a finite distance. In the Theis formula, the constant head boundary was assumed to be at infinity. By looking at Figure 5, both methods yield the same pressure distribution.

Table 1. Aquifer Properties

Permeability (K)	1.06×10^{-10} ft^2
Viscosity (μ)	1.217×10^{-5} lb-sec/ft^2
Porosity (ϕ)	0.39
Density (ρ)	1.938 slug/ft^3
Compressibility Factor (C_F)	0.0 in^2/lb
Density Constant (β)	3×10^{-6} in^2/lb
Bulk Heat Capacity of Water (C_p)	62.4 Btu/ft^3
Bulk Heat Capacity of Rock (C_s)	33.06 Btu/ft^3
Aquifer Depth (D)	50 ft
Initial Pressure (P)	75 ft of water
Grid Angle (θ)	.314 radians
Aquifer Heat Transfer Coefficient (λ)	1.6063 Btu/(hr ft °F)
Top and Bottom Loss Coefficient (h)	0.02847 Btu/(ft^2 °F)

Table 2. Comparison of calculated pressure values and pressures from Theis formula.

Radius (ft)	Pressure - ft (Theis)	Pressure - ft (Calculated)
5.5	86.167	86.189
15	84.864	84.886
30	83.960	83.968
50	83.300	83.323
80	82.685	82.712
150	81.871	81.896
300	80.996	80.995
500	80.306	80.332
800	79.691	79.722
1500	78.878	78.906

The computed temperature distribution paralleled closely to the analytical solution. Figure 6 shows this. There are two reasons why the temperature front spreads out more in the computer solution. The analytical solution assumed no conduction in the radial direction . The only heat flow was by convection and top and bottom losses. Conduction was assumed in the computer model. Also, an effect called smearing will produce a heat front that tends to reach out in front of the hot water.

To determine how depth affects aquifer efficiency, we examined the effect of keeping a constant Q/D ratio. The depth and flow rate were varied. In addition to examining a 100 gpm well 50 ft. deep, a 20 gpm 10 ft. deep aquifer was studied. At this Q/D ratio of 2, injection of 100°F water was carried out for 25 days. Water was then pumped out for

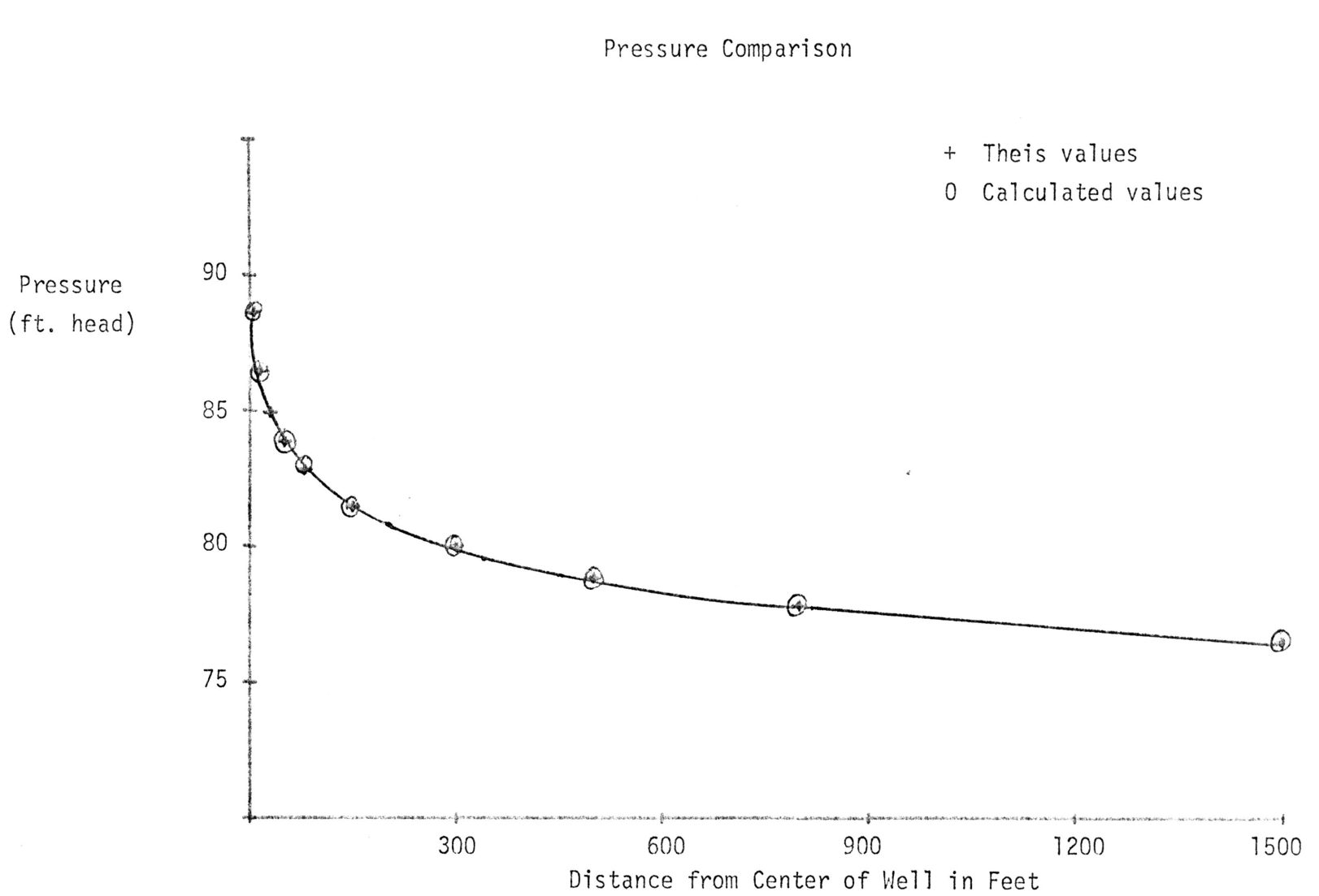

Figure 5. Comparison of Theis pressure values and calculated values.

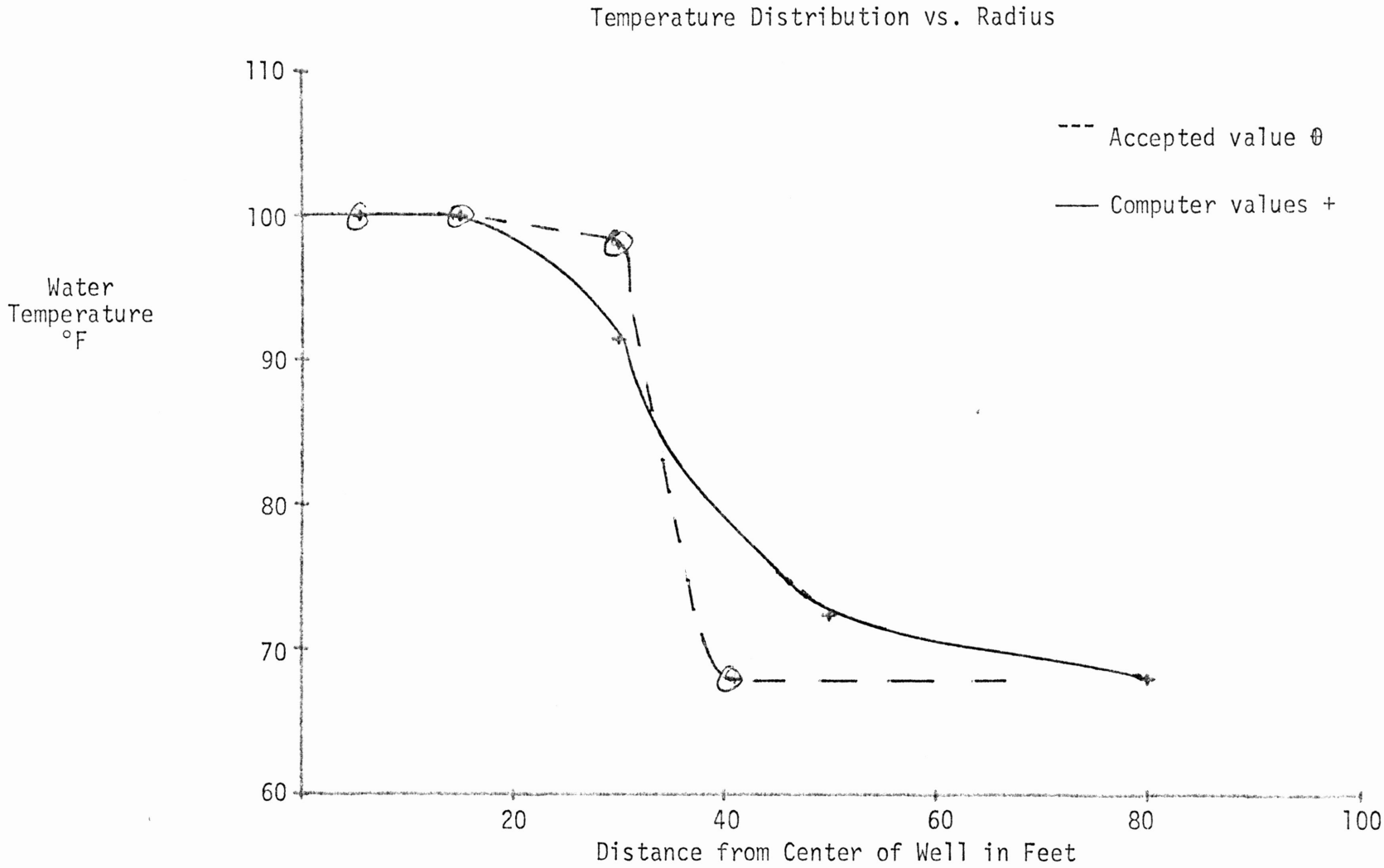

Figure 6. Comparison of accepted values and values for temperature.

25 days. A recovery efficiency was found by dividing the Btu's recovered in pumping by the Btu's pumped in. The recovery efficiency for the 50 ft. aquifer was 78.8% versus 56 for the 10 ft. depth.

The increase in efficiency with depth is due to the energy stored. Five times more energy is stored in the 50 ft. depth as compared to the 10 ft. depth. The losses are a function of the top and bottom area and the temperature difference of the aquifer and bedrock. The areas are the same. The temperature difference is approximately the same and the losses will be about equal. These losses will be a larger percentage in the 10 ft. depth than in the 50 ft. depth.

A second look at the efficiency varying depth was taken with 150°F injected water. The same injection rates and depths were used. The recovery efficiency was 78.8% for the 50 ft. depth compared to 51.6% for the 10 ft. depth. The efficiency difference is caused by the same factors as before.

One important item to look at is the effect of cycles of injecting hot water and pumping this water out. The relationship of efficiency to the number of injection cycles could be of great significance in this process. The cycle looked at was injecting 150°F water at 100 gpm into a 50 ft. aquifer for 30 days. Water was then pumped out for 30 days. The recovery efficiency will hopefully increase with the number of injection cycles. The results of three continuous cycles is shown in Table 3 and Figure 7. The recovery efficiency does increase with cycles and appears to be approaching some value asymptotically. This indicates that part of the energy not pumped is stored in the aquifer. Not as much energy is needed to heat up the aquifer and more can be stored.

Table 3. Injection cycle with recovery efficiency

Aquifer depth	50 ft.	10 ft.
Injection rate	100 gpm	20 gpm
1st cycle		
Btu injected	2.98×10^9	5.95×10^8
Btu recovered	2.34×10^9	3.08×10^8
% recovered	78.8	51.8
2nd cycle		
Btu injected	2.98×10^9	5.95×10^8
Btu recovered	2.43×10^9	3.13×10^8
% recovered	81.8	52.6
3rd cycle		
Btu injected	2.98×10^9	5.95×10^8
Btu recovered	2.45×10^9	3.13×10^8
% recovered	82.4	52.6

Water was injected for 30 days at 150°F and then pumped out for 30 days.

The same thing occurs in the 10 ft. deep aquifer injecting 20 gpm. The efficiencies are not as high as the 50 ft. depth, but there is a small increase from the first to second injection. This aquifer has reached a point of a rather constant efficiency on the third injection. These results indicate using cycles can improve the recovery efficiency of injecting hot water.

The hot water in a usable form is assumed to be 140°F or greater. This water will be hot enough to be used in a heat exchanger and used for

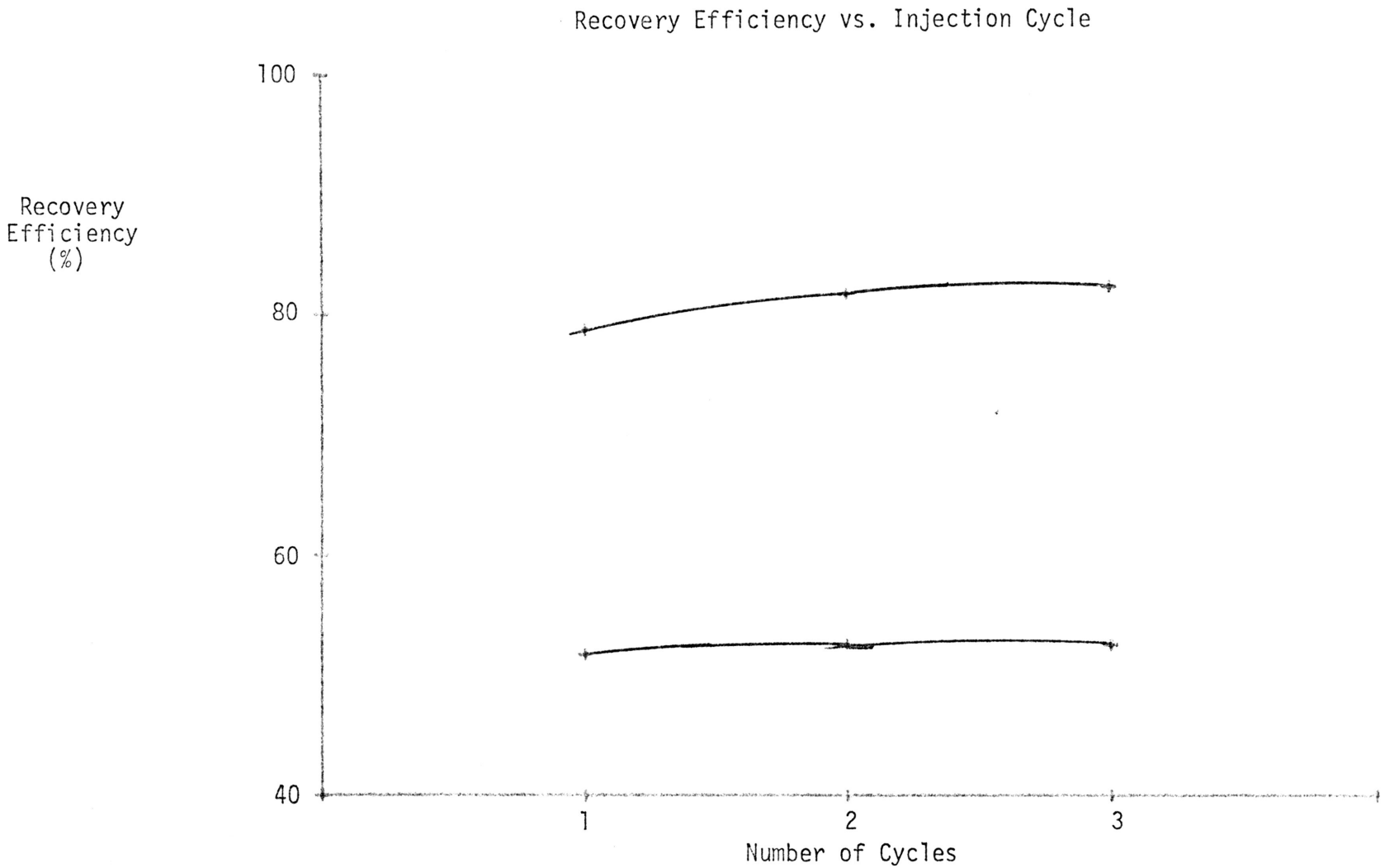

Figure 7. Recovery efficiency with increasing injection cycles.

space heating. After pumping 150°F water at 100 gpm into a 50 ft. deep aquifer, the process was reversed and the water was pumped out. The first 14 days of pumping yielded water at 140°F or greater. The pump out temperature is shown in Figure 8. In this water for the first 14 days, 46% of the energy injected was recovered. Of the 2.98 billion Btu's injected, 1.37 billion were recovered in a form which is easily usable for space heating for one injection cycle.

The energy required for pumping water will only be a small percentage of the energy stored. Assuming a head of 200 ft. is needed to pump 100 gpm, 1.54×10^7 Btu is required for 30 days of pumping. This is only 0.52% of the energy stored. The energy storage will greatly outweigh the pumping costs.

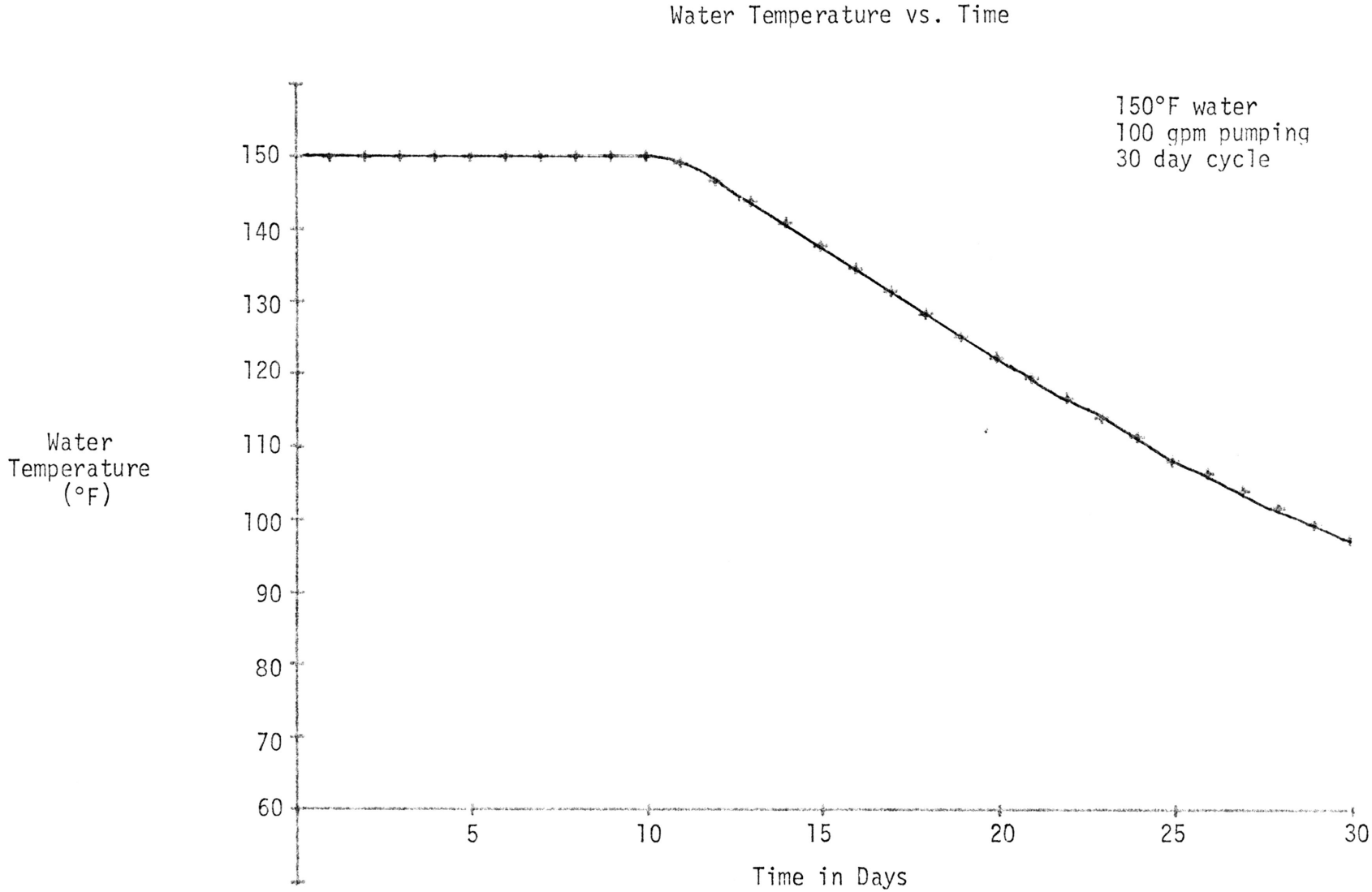

Figure 8. Temperature of water as it is pumped out of well.

CONCLUSIONS

1. The recovery efficiency of an aquifer storage system will increase as the depth of the aquifer increases.

2. The recovery efficiency of an aquifer storage system will increase with continuous injection cycles.

3. Over 40% of the energy injected into an aquifer 50 ft. deep can be reclaimed in an easily usable form of energy.

LIST OF REFERENCES

1. Aziz, K., S. A. Bories, and M. A. Combarnous. 1973. The influence of natural convection in gas, oil, and water reservoirs. Journal of Canadian Petroleum Technology 12:41-47.

2. Castinel, G. and M. A. Combarnous. 1975. Convection naturelle dans une couche poreuse anisotrope. Revue Generale de Thermique. To be published.

3. Combarnous, M. A. and S. A. Bories. 1975. Hydrothermal convection in saturated porous media. Advances in Hydroscience 10:231-307.

4. Gebhart, Benjamin. 1961. Heat Transfer. New York, McGraw-Hill.

5. Gringarten, A. C. and J. P. Sauty. 1975. A theoretical study of heat extraction from aquifers with uniform regional flow. Submitted to the Journal of Geophysical Research for publication.

6. Holman, J. P. 1963. Heat Transfer. New York, McGraw-Hill.

7. Horton, C. W. and F. T. Rogers, Jr. 1945. Convective currents in a porous medium. Journal of Applied Physics 16:367-370.

8. Lapwood, E. R. 1948. Convection of a fluid in a porous medium. Proceedings of Cambridge Phil. Society 44:508-521.

9. Lauwerier, H. A. 1955. The transport of heat in an oil layer caused by the injection of hot fluid. Appl. Sci. Res., Sec. A, 5:145-148.

10. McCray, Arthur W. and Frank W. Cole. 1973. Oil Well Drilling Technology. University of Oklahoma Press, Norman, Oklahoma.

11. Meyer, C. F. and D. K. Todd. 1973. Conserving energy with heat storage wells. Environmental Science and Technology 7(6):512-518.

12. Rabbimov, R. T., R. A. Zhakidov, and G. Ya. Umarov. 1974a. Temperature distribution in accumulation of solar energy in an aquifer. Geliotekhnika 10(2):20-27.

13. Rabbimov, R. T., G. Ya. Umarov, and R. A. Zakhidov. 1974b. Experimental study of aquifer heating in solar-energy accumulation. Geliotekhnika 10(2):20-27.

APPENDIX A

DERIVATION OF THE MASS FLOW EQUATION

The computation for the mass flow equation was based on the following relationship relating to Figure 3.

$$M_{1\to2} - M_{2\to3} = \frac{dM_v}{dt} \tag{A-1}$$

where $M_{1\to2}$ = mass flow into grid 2 across interface A

$M_{2\to3}$ = mass flow out of grid 2 across interface B

$\frac{dM_v}{dt}$ = change of mass in grid 2 with respect to time.

We will only look at the mass flow into grid 2 ($M_{1\to2}$). The outflow ($M_{2\to3}$) can easily be determined after an expression for the inflow is obtained. The mass flow into the grid will be as follows:

$$M_{1\to2} = \rho Q_{1\to2} \tag{A-2}$$

where ρ = density $(\frac{M}{L^3})$

$Q_{1\to2}$ = flow into grid $(\frac{L^3}{T})$.

$$Q_{1\to2} = AV \tag{A-3}$$

where A = cross sectional area (L^2)

V = apparent velocity $(\frac{L}{T})$.

For the grid shown,

$$A = r\Delta\theta D \tag{A-4}$$

where r = radius (L)

$\Delta\theta$ = grid angle

D = aquifer depth (L).

According to McCray (1973), by Darcy's Law:

$$V = -\frac{k}{\mu}\frac{dP}{dr} \tag{A-5}$$

where k = permeability

μ = viscosity

P = pressure.

Substituting (A-3), (A-4), and (A-5) into (A-2) yields

$$M_{1\to2} = \frac{-\rho r \Delta\theta D}{\mu} K \frac{dP}{dr} \tag{A-6}$$

Separating variables and integrating yields

$$\frac{M_{1\to2}\mu}{\rho D \Delta\theta K} \int \frac{dr}{r} - \int dP \tag{A-7}$$

Integrating from $r = r_1$ to $r = r_{1.5}$ and $P = P_1$ and $P = P_{1.5}$ yields

$$\frac{M_{1\to1.5}\,\mu_1}{\rho_1 D_1 \Delta\theta K_1} \ln\left(\frac{r_{1.5}}{r_1}\right) = P_1 - P_{1.5} \tag{A-8a}$$

Integrating from $r = r_{1.5}$ to $r = r_2$ and $P = P_{1.5}$ and $P = P_2$ yields

$$\frac{M_{1.5\to2}\,\mu_2}{\rho_2 D_2 \Delta\theta K_2} \ln\left(\frac{r_2}{r_{1.5}}\right) = P_{1.5} - P_2 \tag{A-8b}$$

By the law of continuity, $M_{1\to1.5} = M_{1.5-2} = M_{1\to2}$. Using this fact and adding (A-8a) and (A-8b) yields

$$M_{1\to2} \left[\frac{\mu_1 \ln\left(\frac{r_{1.5}}{r_1}\right)}{\rho_1 D_1 \Delta\theta K_1} + \frac{\mu_2 \ln\left(\frac{r_2}{r_{1.5}}\right)}{\rho_2 D_2 \Delta\theta K_2}\right] = P_1 - P_2 \tag{A-9}$$

With this, an expression for the flow between points 1 and 2 can be written as a function of aquifer characteristics of each grid point. It is a form of weighted average.

$$M_{1\to2} = \frac{\rho_1\rho_2 D_1 D_2 K_1 K_2 \Delta\theta}{\mu_2\rho_1 D_1 K_1 \ln\left(\frac{r_2}{r_{1.5}}\right) + \mu_1\rho_2 D_2 K_2 \ln\left(\frac{r_{1.5}}{r_1}\right)} (P_1 - P_2) \tag{A-10a}$$

The flow out will be

$$M_{2\to3} = \frac{\rho_2\rho_3 D_2 D_3 K_2 K_3 \Delta\theta}{\mu_3 D_2 K_2 \rho_2 \ln\left(\frac{r_3}{r_{2.5}}\right) + \mu_2 K_3 D_3 \rho_3 \ln\left(\frac{r_{2.5}}{r_2}\right)} (P_2 - P_3) \tag{A-10b}$$

Letting
$$N_1 = \frac{\rho_1\rho_2 D_1 D_2 K_1 K_2 \Delta\theta}{\mu_2 K_1 D_1 \rho_1 \ln(\frac{r_2}{r_{1.5}}) + \mu_1 K_2 D_2 \rho_2 \ln(\frac{r_{1.5}}{r_1})} \quad \text{(A-11a)}$$

$$N_2 = \frac{\rho_2\rho_3 D_2 D_3 K_2 K_3 \Delta\theta}{\mu_3 K_2 D_2 \rho_2 \ln(\frac{r_3}{r_{2.5}}) + \mu_2 K_3 D_3 \rho_3 \ln(\frac{r_{2.5}}{r_{1.5}})} \quad \text{(A-11b)}$$

and substituting into (A-1) yields

$$N_1(P_1-P_2) - N_2(P_2-P_3) = \frac{dM_v}{dt} \quad \text{(A-12)}$$

$$\frac{dM_v}{dt} = \frac{d}{dt}(p\phi r\Delta\theta\Delta rD) \quad \text{(A-12a)}$$

where ϕ = porosity

Δr = change in radius from one interface to another.

The term $r\Delta\theta\Delta rD$ expresses the volume of the grid. The volume of the grid remains constant with time. The density and porosity are functions of pressure which will change with time.

$$\phi = \phi_0 [\ 1 + C_F\ (P - P_0)] \quad \text{(A-13a)}$$

$$\rho = \rho_0 [\ 1 + \beta\ (P - P_0)] \quad \text{(A-13b)}$$

where C_F = rock compressibility factor

β = factor that relates density to pressure.

These expressions show that density and porosity are functions of pressure and therefore a function of time. Taking the derivative of (A-12a) by using the chain rule,

$$\frac{dM_v}{dt} = r\Delta\theta\Delta rD\ [\rho\frac{d\phi}{dt} + \phi\frac{dp}{dt}] \quad \text{(A-14)}$$

Differentiating (A-13a) and (A-13b) with respect to time yields

$$\frac{d\phi}{dt} = \phi_0 C_F \frac{dP}{dt} \quad \text{(A-15a)}$$

$$\frac{d\rho}{dt} = \rho_0 \beta \frac{dp}{dt} \tag{A-15b}$$

Substituting into (A-14)

$$\frac{dM_v}{dt} = \rho_2 \phi r_2 \Delta\theta \Delta r D \, (C_{F_2} + \beta_3) \frac{dP}{dt} \tag{A-16}$$

Letting

$$M_2 = \frac{\rho_2 r \Delta\theta \Delta r D \, (C_F + \beta)}{\Delta t}$$

and putting into finite difference form

$$\frac{dM_v}{dt} = M_2 (P_2{}^{t+\Delta t} - P_2{}^{t}) \tag{A-17}$$

Where the superscripts indicate the time the pressure is to be measured. Combining with (A-12)

$$N_1 (P_1{}^{t+\Delta t} - P_2{}^{t+\Delta t}) - N_2 (P_2{}^{t+\Delta t} - P_3{}^{t+\Delta t}) = M_2 (P_2{}^{t+\Delta t} - P_2{}^{t}) \tag{A-18}$$

This simplifies to

$$N_1 P_1{}^{t+\Delta t} - (N_1 + N_2 + M_2) P_2{}^{t+\Delta t} + N_2 P_3{}^{t+\Delta t} = -M_2 P_2{}^{t} \tag{A-19}$$

This is looking at the 2nd grid point. Looking at the ith grid section, (A-19) becomes

$$N_{i-1} P_{i-1}{}^{t+\Delta t} - (N_{i-1} + N_i + M_i) P_i{}^{t+\Delta t} + N_i P_{i+1}{}^{t+\Delta t} = -M_i P_i{}^{t} \tag{A-20}$$

APPENDIX B

DEVELOPMENT OF HEAT FLOW EQUATIONS

To develop the equations that model the heat flow in an aquifer, we will run a heat balance on grid 2. In determining the heat flow in the groundwater aquifer, we must look at conduction and convection. We began with an equation that parallels (A-1) to deal with the heat flow.

$$Jr_{1\to2} - Jr_{2\to3} = \frac{dH}{dt} \tag{B-1}$$

where $Jr_{1\to2}$ = heat flow in due to conduction and convection

$Jr_{2\to3}$ = heat flow out due to conduction and convection

$\frac{dH}{dt}$ = change in heat stored with time.

$$Jr = -C_F T_q r\Delta\theta D + \lambda r\Delta\theta D \frac{dT}{dr} \tag{B-2}$$

where C_F = specific heat of fluid

T = temperature of fluid (°F)

q = flow rate between the grid points $(\frac{L^3}{T})$

r = radius (L)

$\Delta\theta$ = grid angle

D = aquifer depth (L)

λ = heat transfer coefficient of aquifer

$\frac{dT}{dr}$ = change in temperature with respect to radius.

By Darcy's Law

$$q = -\frac{K}{\mu}\frac{dP}{dr} \tag{B-3}$$

where k = permeability

μ = viscosity

$\frac{dP}{dr}$ = change in pressure with respect to radius.

Substituting this into (B-2) and taking just convection into account,

$$Jr = C_F \, T \, \frac{K}{\mu} \, r\Delta\theta D \, \frac{dP}{dr} \tag{B-4}$$

The term T is an expression for the temperature. The value of T will be dependent on the radius. For ease of calculation, it is assumed that the temperature varies linearly with the radius. This is a form of linear interpolation. Knowing the temperature at the respective radius, the value for the temperature anywhere between these two radius will be

$$T = T_1 - \left(\frac{T_2-T_1}{r_2-r_1}\right)r_1 + \left(\frac{T_2-T_1}{r_2-r_1}\right)r \tag{B-5}$$

where r is at the desired location for calculating T.

Letting $$A_1 = T_1 - \left(\frac{T_2-T_1}{r_2-r_1}\right)r_1 \tag{B-6a}$$

$$B_1 = \frac{T_2-T_1}{r_2-r_1} \tag{B-6b}$$

(B-4) becomes

$$Jr = C_F(A_1+B_1r)\frac{K}{\mu} \, r\Delta\theta D \, \frac{dP}{dr} \tag{B-7}$$

Separating variables and integrating

$$\frac{Jr}{C_F K\Delta\theta D} \, \mu \int \frac{dr}{r(A+Br)} = \int dP \tag{B-8a}$$

$$\frac{Jr}{C_F K\Delta\theta D} \, \mu \ln \frac{r}{(A+Br)} \Bigg| = P \Bigg| \tag{B-8b}$$

Evaluating this from $r = r_1$ to $r = r_{1.5}$, $P = P_1$ and $P = P_{1.5}$ yields

$$\frac{\mu_1 \, Jr}{A_1 C_{F_1} K_1 D_1 D\theta} \ln \frac{r_{1.5}(A+Br_1)}{r_1(A+Br_{1.5})} = P_{1.5} - P_1 \tag{B-9a}$$

Evaluating from $r = r_{1.5}$ to $r = r_2$ and $P = P_{1.5}$ and $P = P_2$

$$\frac{\mu_2 \, Jr}{A_1 C_{F_2} K_2 D_2 \Delta\theta} \ln \frac{r_2(A+Br_{1.5})}{r_{1.5}(A+Br_2)} = P_2 - P_{1.5} \tag{B-9b}$$

Jr in (B-9a) must equal Jr in (B-9b). These both must $Jr_{1\to2}$. With this in mind, the expression for the heat flow in as a function of the properties of each grid will be

$$Jr_{1\to2} = \frac{C_{F_1}C_{F_2}K_1K_2D_1D_2\Delta\theta(P_1-P_2)A_1}{\mu_1K_2C_{F_2}D_2\ \ln\left(\frac{r_{1.5}(A+Br_1)}{r_1(A+Br_{1.5})}\right) + \mu_2K_1C_{F_1}D_1\ \ln\left(\frac{r_2(A+Br_{1.5})}{r_{1.5}(A+Br_2)}\right)} \qquad \text{(B-10a)}$$

This is an expression for the convection heat transfer into the grid. An expression for the heat flow out by convection will be

$$Jr_{2\to3} = \frac{C_{F_2}C_{F_3}K_2K_3D_2D_3\Delta\theta(P_1-P_2)}{\mu_2K_3C_{F_3}D_3\ \ln\left(\frac{r_{2.5}(A+Br_2)}{r_2(A+Br_{2.5})}\right) + \mu_3K_2D_2C_{F_2}\ \ln\left(\frac{r_3(A+Br_{2.5})}{r_{2.5}(A+Br_3)}\right)} \qquad \text{(B-10b)}$$

The variables A and B are functions of the temperature at the grid points. It is impossible to isolate A and B and come up with expressions for the heat flow as an exact function of the temperature. To solve this, the A in the numerator was assumed to be unknown. Let the rest of the expression be

$$x_1 = \frac{C_{F_1}C_{F_2}K_1K_2D_1D_2\Delta\theta(P_1-P_2)}{\mu_1K_2C_{F_2}D_2\ \ln\left(\frac{r_{1.5}(A+Br_1)}{r_1(A+Br_{1.5})}\right) + \mu_2K_1D_1C_{F1}\ \ln\left(\frac{r_2(A+Br_{1.5})}{r_{1.5}(A+Br_2)}\right)} \qquad \text{(B-11)}$$

The values for A and B were originally assumed to be a function of the temperature of the grid at time t. The pressures were those calculated at the end of the time step. The unknown temperatures at time $t+\Delta t$ were found by solving the system of equations using the A in the numerator by remembering

$$A = T_1 - \left(\frac{T_2-T_1}{r_2-r_1}\right) r_1$$

Using this and combining the effects of conduction, the temperatures at the end of the time step could be calculated. Since x_1 is a function of the temperature at time $t+\Delta t$, we must update our coefficient to the end of the time interval and resolve the system of equations. When the

calculated values for temperature and the values used for the coefficients used for x_1 and x_2, the system is solved and the values for the temperatures have been solved:

For convection in and out

$$x_1\left[T_1-\left(\frac{T_2-T_1}{r_2-r_1}\right)r_1\right] - x_2\left[T_2-\left(\frac{T_3-T_2}{r_3-r_2}\right)\right. = \frac{dH}{dt} \tag{B-12}$$

For (B-2) using just conduction

$$Jr = \lambda r \Delta\theta D \frac{dT}{dr} \tag{B-13}$$

Separating variables and integrating

$$\frac{Jr}{\lambda\Delta\theta D}\int \frac{dr}{r} = \int dT \tag{B-14}$$

Integrating from $r = r_1$ to $r = r_{1.5}$

$$\frac{Jr}{\lambda_1\Delta\theta D_1} \ln\left(\frac{r_{1.5}}{r_1}\right) = T_{1.5}-T_1 \tag{B-15a}$$

Integrating from $r = r_{1.5}$ to $r = r_2$

$$\frac{Jr}{\lambda_2\Delta\theta D_2} \ln\left(\frac{r_2}{r_{1.5}}\right) = T_2-T_{1.5} \tag{B-15b}$$

Adding (B-15a) and (B-15b) yields

$$Jr\left[\frac{\ln\left(\frac{r_{1.5}}{r_1}\right)}{\lambda_1\Delta\theta D_1} + \frac{\ln\left(\frac{r_2}{r_{1.5}}\right)}{\lambda_2\Delta\theta D_2}\right] = T_2-T_1 \tag{B-16a}$$

Rearranging, the term for conduction will be

$$Jr_{1\to2} = \frac{\Delta\theta\lambda_1\lambda_2 D_1 D_2 (T_1-T_2)}{\lambda_2 D_2 \ln\left(\frac{r_{1.5}}{r_1}\right) + \lambda_1 D_1 \ln\left(\frac{r_2}{r_{1.5}}\right)} \tag{B-16b}$$

$$Jr_{2\to3} = \frac{\Delta\theta\lambda_2\lambda_3 D_2 D_3 (T_2-T_3)}{\lambda_3 D_3 \ln\left(\frac{r_{2.5}}{r_2}\right) + \lambda_2 D_2 \ln\left(\frac{r_3}{r_{2.5}}\right)} \tag{B-16c}$$

where $Jr_{1\to2}$ is flow in and $Jr_{2\to3}$ is flow out.

Letting
$$y_1 = \frac{\Delta\theta\lambda_1\lambda_2 D_1 D_2}{\lambda_2 D_2 \ln(\frac{r_{1.5}}{r_1}) + \lambda_1 D_1 \ln(\frac{r_2}{r_{1.5}})} \tag{B-17a}$$

$$y_2 = \frac{\Delta\theta\lambda_2\lambda_3 D_2 D_3}{\lambda_3 D_3 \ln(\frac{r_{2.5}}{r_2}) + \lambda_2 D_2 \ln(\frac{r_3}{r_{2.5}})} \tag{B-17b}$$

and substituting into (B-1)

$$y_1 (T_1-T_2) - y_2(T_2-T_3) = \frac{dH}{dt} \tag{B-18}$$

$$\frac{dH}{dt} = (CT \frac{dT}{dt} + \frac{2h}{D} (T_2-T_i))V \tag{B-19}$$

where CT = aquifer bulk heat capacity

V = grid volume

T_i = constant temperature of bedrock and cap rock

h = top and bottom heat loss coefficient.

Substituting (B-12), (B-18), and (B-19) into (B-2)

$$x_1(T_1 - (\frac{T_2-T_1}{r_2-r_1}) r_1) + y_1(T_1-T_2) - x_2(T_2 - (\frac{T_3-T_2}{r_3-r_2}) r_2) -$$

$$y_2(T_2-T_3) = (CT \frac{dT}{dt} - \frac{2h}{D} (T_2-T_i))V$$

Rearranging

$$(y_1 + x_1 + \frac{x_1 r_1}{r_2-r_1}) T_1^{t+\Delta t} - (y_1 + y_2 + x_2 + \frac{x_1 r_1}{r_2-r_1} + \frac{x_2 r_2}{r_3-r_2} +$$

$$\frac{CT\ r_2\Delta\theta D_2\Delta r}{\Delta t} + \frac{2h}{D_2} r_2\Delta\theta\Delta r D_2)T_2^{t+\Delta t} + (y_2 + \frac{x_2 r_2}{r_3-r_2}) T_3^{t+\Delta t} =$$

$$(- \frac{(CT)T_2^t}{\Delta t} - \frac{2h}{D} T_i) V$$

With this expression, the value of the temperature at the end of the time increment can be calculated.